

# Dynamics of dense, charge-stabilized suspensions of colloidal silica studied by correlation spectroscopy with coherent X-rays

Gerhard Grübel,<sup>a</sup> Douglas L. Abernathy,<sup>a</sup> Dirk O. Riese,<sup>b</sup> Willem L. Vos<sup>b</sup> and Gerard H. Wegdam<sup>b</sup>

<sup>a</sup>ESRF, BP220, 38043 Grenoble, France

<sup>b</sup>Van der Waals-Zeeman Institute, U. Amsterdam, 1018 Amsterdam, The Netherlands

Email: gruebel@esrf.fr

The dynamics of concentrated, charge-stabilized colloidal silica suspensions was studied over a wide range of wave-vectors. The short-time diffusion coefficient,  $D(Q)$ , was measured for concentrated suspensions up to their solidification points by photon correlation spectroscopy with coherent X-rays and compared to free particle diffusion  $D_0$ , studied by Dynamic Light Scattering (DLS) in the dilute case. Small angle X-ray scattering (SAXS) was used to determine the static structure factor  $S(Q)$ .  $D_0/D(Q)$  peaks for  $Q$  values corresponding to the maximum of the static structure factor showing that the mostly likely density fluctuations decay the slowest. The data allow one to estimate the diffusion coefficient  $D(Q)$  in the  $Q \rightarrow 0$  and  $Q \rightarrow \infty$  limits. Thus, hydrodynamic functions can be derived free from any modeling of the static or dynamic properties. The effects of hydrodynamic interactions on the diffusion coefficient in charge-stabilized suspensions are presented for volume fractions  $0.075 < \Phi < 0.28$ .

## 1. Introduction

Dynamic Light Scattering (DLS) with visible coherent light from a laser source is a well established technique to investigate the dynamic properties of colloidal suspensions (Pusey, 1989). DLS, also known as photon correlation spectroscopy, is based on a very prominent feature, occurring whenever coherent light is scattered from a random medium. There are strong spatial modulations of the scattered intensity, called a speckle pattern, resulting from the summing of the randomly phased electric fields from the individual scatterers in the medium. If the spatial arrangement of scatterers changes in time the corresponding speckle pattern will also change and a measurement of the intensity fluctuations at a point in the far field can reveal the dynamics of the system. Photon correlation spectroscopy in the visible is however subject to two main limitations: (i) the occurrence of multiple scattering in opaque systems (e.g. concentrated colloidal suspension) considerably complicates the interpretation of the experiments, (ii) the use of visible light prevents the dynamics to be traced on length scales smaller than about 2000 Å. Both limitations can be surmounted by correlation spectroscopy with coherent X-rays (DXS) provided by a synchrotron source. DXS is a novel technique that only recently has started to be applied to colloidal systems (Dierker et al., 1995; Thurn-Albrecht et al., 1996; Tsui & Mochrie, 1998) including free particle diffusion in a dilute suspension of colloidal silica (Grübel et al., 1999). We have studied the static and dynamic properties of dense, charge-stabilized colloidal silica suspensions by scattering with coherent X-rays. Combined

with the results of the measurement of the diffusion coefficient in the zero density limit we determine the hydrodynamic interaction over the relevant wave-vector range free from any modeling of the static or dynamic properties.

Correlation spectroscopy determines the dynamic properties of matter by measuring the temporal correlations in the fluctuations of the intensity scattered by the sample. Correlations can be quantified via the normalized time correlation function

$$g(Q,t) = \langle I(Q,0) I(Q,t) \rangle / \langle I \rangle^2 = 1 + A(Q) |f(Q,t)|^2, \quad (1)$$

where  $I(Q,t)$  is the scattered intensity at wave-vector  $Q$  and the angular brackets denote the average.  $A(Q)$  is a function depending on the coherence properties of the source and typical values range between 0.1 and 0.25 in the X-ray case. The function  $f(Q,t)$  denotes the normalized intermediate scattering function also known from quasielastic light or neutron scattering. The simplest functional form for a translational diffusion process is an exponential

$$f(Q,t) = \exp(-D(Q) Q^2 t), \quad (2)$$

where  $D(Q)$  is the diffusion coefficient. The exponential decay of temporal correlations is illustrated in Fig. 1 showing a DXS measurement (open circles) of the intermediate scattering function of a sample of colloidal silica suspended in a mixture of glycerol/water with a refractive index of 1.42 for visible light, making the sample opaque to the eye. The result of a DLS measurement from the same sample is shown for comparison. The DLS intermediate scattering function (closed squares) relaxes faster as a result of multiple scattering since the light wave scatters from more than one moving particle. It hence suffers a larger phase shift and the correlation is lost faster than for single scattering. Although the characteristic square root dependence of  $f(Q,t)$  on time, known from diffusive wave spectroscopy (Pine et al., 1990), is not yet observed one readily realizes that the correlation time is already affected. The DXS data are not subject to multiple scattering effects since the refractive index for X-rays is always very close to one. DLS and DXS results are identical in the absence of multiple scattering in perfectly index-matched samples. A detailed discussion of multiple scattering effects will be given in a forthcoming paper (Riese et al., 2000).

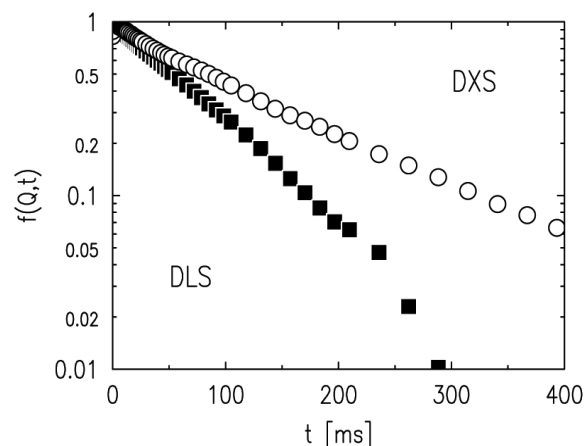


**Figure 1** Intermediate scattering functions  $f(Q,t)$  measured by DXS (open circles) and DLS (closed squares) at  $Q=0.0009 \text{ \AA}^{-1}$  in an optically opaque sample of colloidal silica (1820 Å radius) suspended with a volume fraction of  $\Phi=0.09$  in a glycerol/water solvent.

In the dilute case ( $\Phi \ll 1$ ) the colloidal particles migrate driven by the thermal fluctuations of the solvent, with a diffusion coefficient given by the Stokes-Einstein relation,

$$D(Q) = D_0 = kT / 6\pi\eta R_h, \quad (3)$$

where  $D_0$  is the (free particle) diffusion coefficient,  $k$  is the Boltzmann constant,  $T$  the temperature,  $\eta$  the viscosity of the solvent and  $R_h$  the hydrodynamic radius of the diffusing particle.

At larger concentrations, interparticle interactions as well as indirect, hydrodynamic interactions, mediated by the solvent become important. Then, the short-time ( $t < R^2/D_0$ ) behaviour of the intermediate scattering function can be described by a wave-vector dependent diffusion coefficient

$$D(Q) = D_0 H(Q) / S(Q), \quad (4)$$

where  $H(Q)$  is the hydrodynamic function and  $S(Q)$  the structure factor (Hansen & McDonald, 1986). The slowing down of the diffusion around the peak in  $S(Q)$  is by now well established and is often referred to as the cage effect. However it is still an open question how the diffusion behaves in the small and large wave-vector limits. For large  $Q$  one expects the colloidal particle to perform a random walk inside the cavity formed by the surrounding particles. For hard spheres theory predicts  $H(Q \rightarrow \infty) \leq 1$ . To date there are no measurements to assess the influence of the direct and hydrodynamic interactions on the diffusion process in this wave-vector regime.

For light scattering the determination of  $D(Q)$  and  $S(Q)$  over a large wave-vector range is a formidable task. The requirement of index matching to suppress multiple scattering has limited the DLS measurements to hard-sphere and/or low density systems. A consistent picture has nevertheless emerged for hard-sphere fluids by a combination of experimental DLS data and hard-sphere calculations of the form and structure factors. The availability of analytical expressions for the structure factor of the hard-sphere fluid within the Percus-Yevick approximation (Hansen & McDonald, 1986) and the calculations of hydrodynamic functions by Beenakker and Mazur (1984) were essential for the interpretation of the data. For charge stabilized colloidal systems the situation is more complicated. For these systems only numerical models for the structure factor exist: the mean spherical approximation MSA (Hayter & Penfold, 1981) or the rescaled RMSA version (Hansen & Hayter, 1982). Hydrodynamic effects in charged colloidal suspensions have been calculated for the monodisperse case (Genz & Klein, 1991) and for polydisperse systems (Nägele et al., 1993). Experimental attempts to study interacting, charge-stabilized systems are however scarce (Philipse & Vrij, 1988; Phalakornkul et al., 1996).

## 2. Experimental details

The experiments were carried out at beamline ID10A (Grübel & Abernathy, 1997; Abernathy et al., 1998) of the European Synchrotron Radiation Facility (ESRF) with X-rays of 8.2 keV (1.51 Å) energy, supplied by a single bounce Si(111) monochromator. A vertically focussing Rh-coated Si mirror was set to a critical energy just above 8.2 keV for harmonics rejection. The nominal transverse coherence lengths  $\xi_{\perp} = \lambda R_s / 2\sigma$  were 144  $\mu\text{m}$  (vertically) and 13  $\mu\text{m}$  (horizontally) at a distance  $R_s = 44\text{m}$  from the source

**Table 1**

Summary of quantities obtained from static SAXS characterization.

Volume Fraction $\phi$	Average radius $R[\text{Å}]$	Size polydispersity $\Delta R/R$	Location of first S(Q) peak $Q_0 R$
0.075	561	0.017	2.41
0.15	555	0.035	2.47
0.28	481	0.150	2.79

with size  $\sigma$ . A partially coherent X-ray beam was selected by placing a  $d=20\ \mu\text{m}$  collimating pinhole aperture 0.8m downstream of the mirror. The longitudinal coherence length  $\xi_{\parallel} = \lambda / \Delta\lambda = 1\ \mu\text{m}$  was determined by the bandpass  $\Delta\lambda/\lambda = 1.4 \cdot 10^{-4}$  of the Si(111) monochromator. Coherent illumination of the sample volume requires that the maximum pathlength difference  $(d^2 \sin^2 2\theta + h^2 [1 - \cos 2\theta])^{1/2} \leq \xi_{\parallel}$  for rays scattered at an angle  $\theta$  in transmission through a sample with thickness  $h$  ( $=1\text{mm}$ ). This is the case for  $Q < 0.15\ \text{Å}^{-1}$  and is sufficient for the present measurements. Experiments at even larger wave-vectors are possible but might require a higher monochromaticity of the beam and the use of fast 2-D detectors. The samples were positioned 0.13m downstream of the collimating aperture in an evacuated chamber connected to a drift tube. A guard slit was positioned right in front of the sample capillaries to eliminate parasitic scattering from the collimating aperture. In order to detect intensity fluctuations the detector aperture has to be comparable to the angular size  $\lambda/d$  of the speckles. An analysing aperture of 30  $\mu\text{m}$  size was used in front of a scintillation counter at a distance of 1.4 m from the sample and correlation functions were recorded with a digital autocorrelator. The SAXS data were taken in the same configuration.

DLS data were taken with a standard set-up including a diode pumped, frequency doubled Nd:YAG laser with an output of 100 mW at  $\lambda=5320\ \text{Å}$ . Polarizers were inserted to observe just the VV component of the scattering with a photomultiplier connected to the autocorrelator.

The colloidal silica particles were synthesized by polymerization in a microemulsion or by Stöber synthesis. The dilute stock suspension in pure ethanol was centrifuged to reduce the solvent content and resuspended in an ethanol-58 vol% benzylalcohol mixture with refractive index  $n=1.465$  matching the refractive index of the silica particles. A concentrated master suspension (about 40 vol%) was prepared by centrifugation and a series of samples with intermediate volume concentrations were prepared by diluting with known amounts of liquid. Samples from different batches with the characteristics listed in table 1 were used.

## 3. Results and discussion

Structural information in terms of size, shape, size polydispersity and interparticle correlations were obtained by SAXS measurements in the concentrated and dilute suspensions. The scattering cross section may be described by

$$(d\sigma/d\Omega)/V = r_0^2 n_p v_p^2 (\rho_c - \rho_s)^2 |F(Q)|^2 S(Q) \quad (5)$$

where  $r_0$  is the Thompson radius,  $n_p$  is the number concentration of particles,  $\rho_c$  and  $\rho_s$  are the electronic densities of the colloidal particle and of the solvent respectively and  $v_p$  is the particle volume. The form factor  $F(Q)$  for a sphere of radius  $R$  is given by  $F(QR) = 3[(\sin(QR) - QR \cos(QR)) / (QR)^3]$  and size polydispersity  $\Delta R/R$  was taken into account by convolution with a Schultz distribution. The

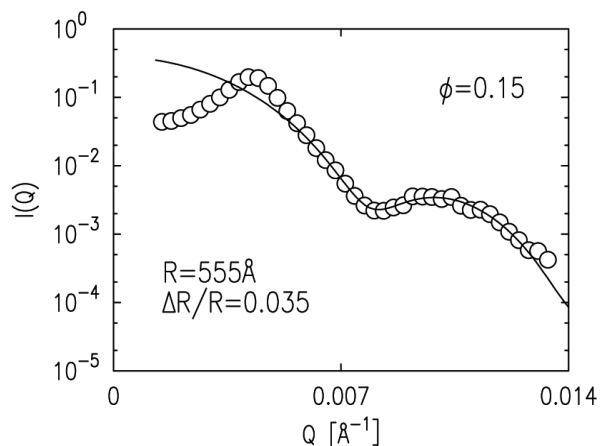


**Figure 2**  
Scattering intensity as a function of wave-vector transfer  $Q$  of a  $\Phi=0.15$  suspension of colloidal silica particles ( $R=555\text{\AA}$ ,  $\Delta R/R=0.035$ ) in ethanol/benzylalcohol. The solid line is a fit to the data based on the form factor of a sphere.

finite detector resolution was taken into account by convolution with a box shaped resolution function. Data from a concentrated sample ( $\Phi=0.15$ ) are shown in Fig. 2. The solid line is a fit of eq. 5 to the data based on the parameters for the dilute case ( $R=555\text{\AA}$ ,  $\Delta R/R=0.035$ ) and assuming  $S(Q)=1$ . The structure factor is extracted by dividing the intensities  $I(Q)$  by their values for the respective dilute samples. The resulting static structure factors  $S(Q)$  are shown in Fig. 3 (open symbols) as a function of  $QR$  for three different volume concentrations. The  $S(Q)$  curves oscillate in all cases to one at high  $Q$  values (not shown). The positions of the structure factor maxima shift to higher wave-vectors when the concentration is increased and the respective peak values increase as expected, except for the highest concentration ( $\Phi=0.28$ ). This is caused by the higher size polydispersity ( $\Delta R/R=0.15$ ) of this sample.

The observed structure factors cannot be described within a hard-sphere model. This is illustrated for the  $\Phi=0.15$  sample in Fig. 3 (middle) by the dashed line showing the calculated hard-sphere structure factor for  $R=555\text{\AA}$ ,  $\Delta R/R=0.035$ . It clearly fails to describe the data. Not just the position, but also the shape distinctly differs from the calculated hard-sphere result. Further modelling of the static data was not attempted within the scope of this paper, but will be discussed in a forthcoming publication.

The dynamic data were all taken on index matched samples using an ethanol-benzylalcohol solvent. Dilute suspensions were measured by DLS to determine the free particle diffusion coefficient  $D_0$ . The concentrated suspension were measured with DXS. One sample ( $\Phi=0.15$ ) was also studied by DLS, but the restricted  $Q$  range ( $Q < 2.4 \cdot 10^{-3} \text{\AA}^{-1}$ ) does not allow to access the regime of the structure factor peak. The DXS data were corrected for the known time structure of the synchrotron beam and the diffusion coefficients were extracted by fitting eq. (2) to the short-time regime of the correlation functions. The normalized inverse diffusion coefficient  $D_0/D(Q)$  was determined by dividing the dilute (DLS) data by the  $D(Q)$  values from the concentrated samples. The results are plotted in Fig. 3 (solid symbols) as a function of  $QR$ . Fig. 3 (middle) demonstrates that DLS and DXS data perfectly superimpose for index-matched samples. At higher  $Q$ , a pronounced peak is observed that coincides in position with the maximum of the static structure factor  $S(Q)$ . Maxima in  $D_0/D(Q)$  are observed for all three concentrations with ampli-

tudes that increase with increasing volume fraction. The positions of the  $D_0/D(Q)$  maxima mimic the behaviour of the static structure factor and shift also to higher wave-vectors with increasing concentration, consistent with eq. (4). This confirms that the most likely density fluctuations, the ones measured at the structure factor peak, are the ones that decay the slowest.

The collective diffusion coefficient  $D_c=D(0)$  (i.e. the  $Q \rightarrow 0$  limit of  $D(Q)$ ) is finite and  $D_0/D_c$  ranges between 0.2 and 0.7. The large- $Q$  diffusion coefficient  $D(\infty)$  can be qualitatively estimated from the data for  $QR > 3.5$ . It is smaller than the free particle diffusion coefficient ( $D(\infty) < D_0$ ) and  $D(\infty)$  decreases with increasing volume fraction. This is expected with similar values for both charged and hard-sphere systems (Nägele et al., 1993). The prediction for the

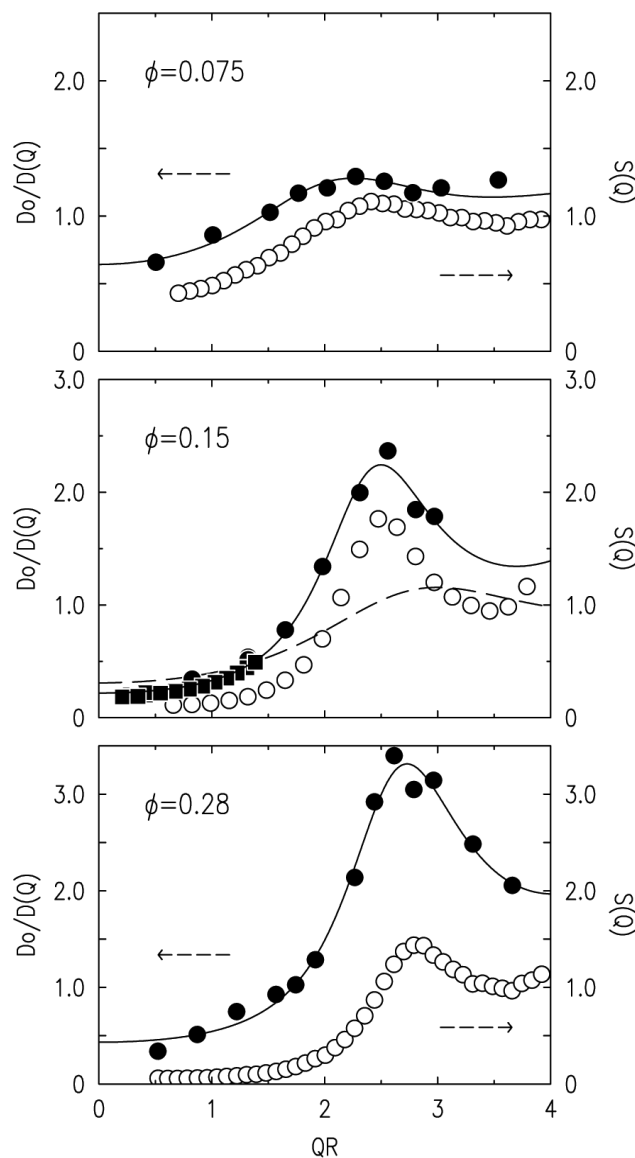


**Figure 3**  
Static structure factor  $S(Q)$  for suspensions of colloidal silica with volume fractions  $\Phi=0.075$ ,  $0.15$  and  $0.28$  (open symbols). The dashed line (middle) represents the calculated hard-sphere structure factor. Normalized inverse diffusion coefficient  $D_0/D(Q)$  taken by DXS (closed circles) and DLS (closed squares). The solid lines are guides to the eye.

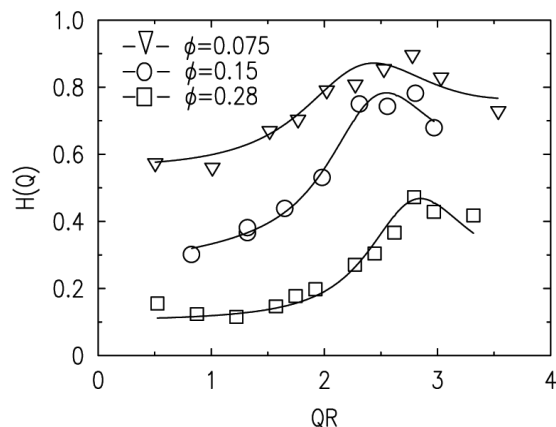


**Figure 4**

Hydrodynamic functions  $H(Q)$  for charge-stabilized colloidal silica for three different concentrations ( $\Phi=0.075, 0.15$  and  $0.28$ ). The solid lines are guides to the eye.

hard-sphere case is  $D_0/D(\infty) = (1 - 1.72\phi + 0.88\phi^2)^{-1} = 1.14, 1.31$  and  $1.71$  for  $\phi=0.075, 0.15$  and  $0.28$ , respectively. This is compatible with the measured data. It is evident from Fig. 3 that  $D_0/D(Q) > S(Q)$  indicating that hydrodynamic interactions are relevant for the investigated system.

Hydrodynamic interactions have been quantified by calculating the ratio between  $D_0/D(Q)$  and  $S(Q)$  and the results are shown in Fig. 4. The  $H(Q)$  functions are reminiscent of the hydrodynamic functions calculated by Beenakker and Mazur (1984) for hard spheres. We find that  $H(Q) < 1$  for all samples and decreasing with increasing volume concentration. This is intuitively expected if hydrodynamic interactions are regarded as additional “friction” further slowing down the dynamics. The observed behaviour however clearly differs from earlier DLS work in moderately concentrated ( $\phi < 0.1$ ), charge-stabilized silica (Philipse & Vrij, 1988; Phalakornkul et al., 1996), where the peaks in the hydrodynamic functions were reported to increase with concentration to values even above one. The shape of the functions in Fig. 4 appears asymmetric and skewed towards the high- $Q$  side. This would indicate, as expected, that the long wavelength modes ( $Q < Q_0$ ) are damped stronger than the short wavelength ones. A further quantitative analysis will require input from a theory addressing the hydrodynamic behaviour of a charge stabilized system at elevated concentrations. The experiment described here establishes

quantitatively and directly the hydrodynamic functions  $H(Q)$  over the whole relevant wave-vector range without taking recourse to any modeling of the static or dynamic properties.

## References

- Abernathy, D.L., Grübel, G., Brauer, S., McNulty, I., Stephenson, G.B., Mochrie, S.G.J., Sandy, A.R., Mulders, N. & Sutton, M. (1998). *J. Synchrotron Rad.* **5**, 37-47.
- Beenakker C.W.J. & Mazur, P. (1984). *Physica* **126A**, 349-370.
- Dierker, S.B., Pindak, R., Fleming, R.M., Robinson, I.K. & Berman, L. (1995). *Phys. Rev. Lett.* **75**, 449-452.
- Genz, U. & Klein, R. (1991). *Physica* **171**, 26-42.
- Grübel, G. & Abernathy, D.L. (1997). *Coherent Electron-Beam X-Ray Sources: Techniques and Applications*, Vol. **3154**, edited by A.K. Freund, H.P. Freund & M.R. Howells, pp. 103-109. SPIE-Int. Soc. Opt. Eng.
- Grübel, G., Robert, A. & Abernathy, D.L. (1999). *Slow Dynamics in Complex Systems*, Eighth Tohwa University International Symposium, edited by M. Tokuyama & I. Oppenheim, pp. 158-159.
- Hansen, J.P. & Hayter, J.B. (1982). *Mol. Phys.* **46**, 651-656.
- Hansen, J.P. & McDonald, I.R. (1986). *Theory of Simple Liquids*, New York: Academic Press.
- Hayter, J.B. & Penfold, J. (1981). *Mol. Phys.* **42**, 109-118.
- Nägele, G., Kellerbauer, O., Krause, R. & Klein, R. (1993). *Phys. Rev. E* **47**, 2562-2574.
- Phalakornkul, J.K., Gast, A.P., Pecora, R., Nägele, G., Ferrante, A., Mandl-Steininger, B., & Klein, R. (1996). *Phys. Rev. E* **54**, 661-675.
- Philipse, A.P. & Vrij, A. (1988). *J. Chem. Phys.* **88**, 6459-6470.
- Pine, D.J., Weitz, D.A., Maret, G., Wolf, P.E., Herbolzheimer, E. & Chaikin, P.M. (1990). *Scattering and Localization of Classical Waves in Random Media*, edited by P. Sheng, pp. 312-372. Singapore: World Scientific.
- Pusey, P.N. (1989). *Liquids, Freezing and Glass Transition*, edited by J.P. Hansen, D. Levesque and J. Zinn-Justin, Les Houches, Session L1, pp. 763-941. Amsterdam:Elsevier.
- Riese, D.O., Vos, W.L., Wegdam, G.H., Poelwijk, F.J., Abernathy, D.L. & Grübel, G. (2000). *Phys. Rev. E* **61**, in print.
- Thurn-Albrecht, T., Steffen, W., Patkowski, A., Meier, G., Fischer, E.W., Grübel, G. & Abernathy, D.L. (1996). *Phys. Rev. Lett.* **77**, 5437-5440.
- Tsui, O.K.C. & Mochrie, S.G.J. (1998). *Phys. Rev. E* **57**, 2030-2034.